Acta Pharmaceutica Sinica B 2019;9(1):118–127

Chinese Pharmaceutical Association
Institute of Materia Medica, Chinese Academy of Medical Sciences

Acta Pharmaceutica Sinica B

www.elsevier.com/locate/apsb
www.sciencedirect.com

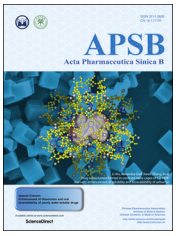

ORIGINAL ARTICLE

Development of carrier-free nanocrystals of poorly water-soluble drugs by exploring metastable zone of nucleation ☆

Xiaoting Ren[a], Jianping Qi[b], Wei Wu[b], Zongning Yin[a,], Tonglei Li[c,***], Yi Lu[b,*]**

[a]*Key Laboratory of Drug Targeting and Drug Delivery Systems, West China School of Pharmacy, Sichuan University, Chengdu 610041, China*
[b]*Department of Pharmaceutics, School of Pharmacy, Fudan University, Shanghai 201203, China*
[c]*Department of Industrial and Physical Pharmacy, College of Pharmacy, Purdue University, West Lafayette, IN 47907, USA*

Received 16 February 2018; received in revised form 27 March 2018; accepted 12 April 2018

KEY WORDS

Nanocrystals;
Metastable zone;
Nucleation;
Sonication;
Dissolution;
Paclitaxel

Abstract There has been increasing interest in research and development of nanocrystals for the delivery of poorly water-soluble drugs that can be directly produced from solution. Compared with traditional carrier-based or encapsulation designs, drug nanocrystals circumvent possible side-effects due to carrier polymers and poor stability issues associated with encapsulation. The production of carrier-free nanocrystals requires careful control of nucleation and thus a thorough understanding of the relevant solution's metastable zone. A solution may stay supersaturated without forming any nuclei and become metastable. The maximal degree of supersaturation is known as the metastable zone width. When nucleation is triggered directly from the metastable zone, it helps to produce homogeneous nuclei leading to uniform nanocrystals. Herein, we report a study in which the solubility and metastable limit of paclitaxel (PTX) in ethanol aqueous solution were measured at 40 °C. A wide range of metastable compositions were studied to prepare carrier-free PTX nanocrystals with particle size smaller than 250 nm and PDI less than 0.25. Compared with the raw material, dissolution rate of PTX nanocrystals was significantly increased. The study enables production of high-quality drug nanocrystals for treating patients.

*Corresponding Author at: Department of Pharmaceutics, School of Pharmacy, Fudan University, 826 Zhangheng Road, Shanghai, 201203, China.
**Corresponding Author at: Key Laboratory of Drug Targeting and Drug Delivery Systems, West China School of Pharmacy, Sichuan University, Chengdu, 610041, China.
***Corresponding Author at: Department of Industrial and Physical Pharmacy, College of Pharmacy, Purdue University, West Lafayette, IN 47907, USA.
E-mail addresses: fd_luyi@fudan.edu.cn (Yi Lu), yzn@scu.edu.cn (Zongning Yin), tonglei@purdue.edu (Tonglei Li).
☆Invited for Special Column.
Peer review under responsibility of Institute of Materia Medica, Chinese Academy of Medical Sciences and Chinese Pharmaceutical Association.

https://doi.org/10.1016/j.apsb.2018.05.004

1. Introduction

Drug nanocrystals are pure drug crystals with a particle size generally smaller than a few hundreds of nanometers[1,2]. Size reduction to the nanometer range leads to significantly increased surface area and thus facilitates dissolution. Nanocrystal formulations have been mainly developed for oral delivery of poorly soluble drugs, improving oral bioavailability and minimizing pharmacokinetic variability[3,4]. Many nanocrystal-based oral drug products have been successfully marketed[5]. Most of these products employ drug nanocrystals that are produced by the top-down approach, that is, by milling larger drug crystals. In order to reduce the size and maintain the size distribution of nanocrystals, surfactants are typically required to treat the surface of the nanocrystals, raising safety concerns due to the surfactant-induced side effects[6]. In addition, the use of stabilizer materials increases the overall chemical burden to patient; the drug-loading becomes correspondingly reduced, further exacerbating potential toxic reactions.

Anti-solvent methods have been used to prepare pure nanocrystals without addition of stabilizers during crystallization[7–11]. Pure paclitaxel (PTX) and camptothecin nanocrystals with average particle sizes ranging from 200 to 500 nm have been produced by mixing the drug solution with a poorly miscible solvent or anti-solvent. The anti-solvent crystallization approach is apparently achieved by reaching supersaturation because of mixing with the anti-solvent and subsequently triggering solid precipitation. Ideally, during the mixing process, nucleation is avoided and the mixture reaches the metastable limit, followed by abrupt and simultaneous phase transition. The more nuclei formed in the nucleation stage, the less growth of each nucleus and more uniformity achieved by the resultant nanocrystals[12–14]. Clearly, ensuring nucleation triggered simultaneously throughout the solution is crucial to produce small, uniform nanocrystals from solution. A probable method is to induce nucleation at the contact of two mixing liquid streams of the drug solution and anti-solvent. However, this approach often results in particles of different sizes and, eventually, fewer and larger crystals (due to Ostwald's Ripening).

Nucleation triggered at the limit of the solution's metastable zone (Fig. 1) may be a useful approach to control particle size. Although crystallization from the metastable zone has been widely studied to understand the nucleation mechanism[15–18], it has not been systemically examined for the purpose of nanocrystal preparation. Shown in Fig. 1, a solution can stay supersaturated without forming any nuclei and remain in the metastable state. In order to achieve a maximum nucleation rate, the metastable limit needs to be approached as closely as possible. Ultrasound may serve as a driving force for triggering nucleation in the metastable state[19–21], by creating tiny vapor bubbles in solution, whose collapse may lead to intense shock waves (*i.e.*, cavitation effect)[19]. The bubble explosion results in extremely rapid and localized temperature reduction in solution, while the shock waves facilitate mass transfer[22]. Altogether, the nucleation rate is increased, leading to the formation of small, uniform nanocrystals.

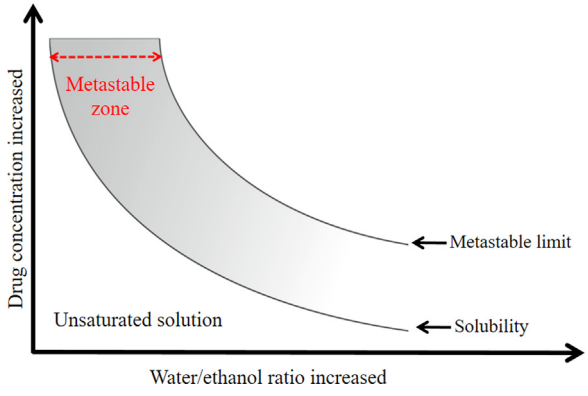

Figure 1 Illustration of metastable zone.

In this study, we measured the metastable zone of PTX in water and ethanol mixtures and conducted nanocrystal productions under various conditions. PTX is a chemotherapeutic compound, often given by intravenous injection. However, to improve the quality of life and cut health care costs, oral delivery of chemotherapeutic drugs has been actively considered, including several drug products marketed for the oral route[23–25]. Around 25% of cancer chemotherapy is administrated as an oral formulation as of 2013[24]. Since more than 40% of anticancer drugs are water-insoluble[26], carrier materials were generally utilized to solubilize and/or encapsulate drug substances into various dosage forms (*e.g.*, solutions, micelles, liposomes, and nanoparticles) in order to improve oral bioavailability[27–31]. Given the aforementioned disadvantages of carrier materials, carrier-free nanocrystals offer numerous benefits for oral delivery of chemotherapeutic compounds. Herein, carrier-free PTX nanocrystals were prepared by nucleation triggered from the metastable zone. The dissolution of PTX by nanocrystals was also studied.

2. Materials and methods

2.1. Materials

Paclitaxel (>99.5%, USP30) was purchased from Meilun Biotechnology Co., Ltd. (Dalian, China). Ethanol and Tween 80 were purchased from Sinopharm Chemical Reagent Co., Ltd. (Shanghai, China). Acetonitrile (Tedia Company, Inc., Fairfield, OH, USA) was of high performance liquid chromatography (HPLC) grade. Deionized water was prepared by a Mili-Q water purifying system (Millipore, Bedford, MA, USA).

2.2. PTX content measured with HPLC

PTX concentration was measured by Agilent 1260 series HPLC system (Agilent Technologies Inc., Santa Clara, CA, USA). PTX was separated through a Zorbax C18 column (5 μm, 150 mm × 4.6 mm, Agilent Technologies Inc., Santa Clara, CA, USA) heated at 40 °C. The mobile phase, a mixture of acetonitrile and water (50:50), was pumped at a flow rate of 1.0 mL/min. Sample solution, 20 μL, was injected and detected at 227 nm. The retention time of PTX was around 4.4 min. Within the concentration range of 2.008–100.40 μg/mL, the PTX concentration (C) is linear with its peak area (A) with a typical calibration curve of $C=0.049A-0.238$, $r^2=0.9999$.

2.3. Solubility of PTX

Excess amount of PTX powders was suspended in 5, 10, 20, 30, 40, 50, 60 and 70% (*v*/*v*) ethanol aqueous solutions, respectively. The suspensions were stirred with electromagnetic stirring (RCT basic, IKA, Staufen, Germany) at 200 rpm and kept in water bath at 40 °C. After 24 h, the suspensions were filtered with 0.45 μm

membranes (Xinya purification device factory, Shanghai, China). The filtrates were diluted 1- to 100-fold with ethanol for HPLC measurement. The dilution prevented PTX precipitation due to temperature variation and ensured sampling concentrations within the linear range of the standard curve.

2.4. Measurement of metastable zone width

Based on the solubility curve, the metastable limit of PTX in ethanol aqueous solution at 40 °C was measured in a crystallizer with modification[32,33]. The saturated PTX in different ethanol aqueous solutions were kept at 40 °C and stirred by magnetic stirring bar at 200 rpm. Pure water of equal temperature was instilled, 160 μL/min, by a syringe pump (BASi, Bioanalytical Systems Inc., West Lafayette, IN, USA) into the saturated solution. A laser beam was passed through the solution to observe any formation of nuclei (*i.e.*, Tyndall effect). The amount of water added was recorded when nuclei were detected. Then the metastable limit was derived based on the PTX amount and ethanol/water ratio.

2.5. Preparation of nanocrystals by nucleation from metastable solution

From the metastable limit measured, a specified amount of PTX was dissolved in ethanol, and agitated at 200 rpm at a temperature of 40 °C. Water of equal temperature was then instilled using a syringe pump at 160 μL/min to achieve a metastable, supersaturated solution. Subsequently, sonication (SB-5200D, Ningbo Scientz Biotechnology Co., Ltd., Ningbo, China) was performed to the metastable solution to trigger nucleation. After a period of time, the suspensions were filtered through 50 nm Whatman® Nuclepore polycarbonate track-etched membrane (GE Healthcare Life Sciences, Pittsburgh, PA, USA). The filter cake was redispersed in 5 mL pure water with the aid of sonication to obtain final nanocrystals. The composition of the metastable solution was screened according particle size and polydispersity index (PDI) of the obtained nanocrystals. Then, the sonication time in the nucleation and redispersion stage was optimized, respectively.

2.6. Yield of nanocrystals and recovery of PTX

The obtained nanocrystal suspensions, 1 mL, were dissolved and diluted by acetonitrile to 5 mL, 20 μL of which was injected to HPLC for measurement of PTX concentration. The amount of nanocrystals (W_{nano}) can be calculated through the dilution folds. The yield of nanocrystals (Y) was calculated by the following Eq. (1):

$$Y = \frac{W_{nano}}{W_{total}} \times 100\% \quad (1)$$

where W_{total} is the total amount of PTX added to prepare nanocrystals.

PTX can be solubilized in the solution and removed by filtration. The recovery of PTX includes two parts, collected nanocrystals and dissolved free drug in the filtrate. Therefore, the filtrate was collected and diluted to 25 mL with acetonitrile. The solution, 20 μL, was injected to HPLC for measurement of PTX amount in the filtrate (W_f). Recovery of PTX (R) was calculated by the following Eq. (2):

$$R = \frac{W_{nano} + W_f}{W_{total}} \times 100\% \quad (2)$$

2.7. Characterization

2.7.1. Particle size

Malvern Zetasizer Nano® instrument (Malvern Instruments, Malvern, UK) was used to determine the particle size and PDI of PTX nanocrystals. The Zetasizer was equipped with a 4 mW He-Ne laser (633 nm). Samples were directly measured without any dilution and were balanced for 120 s in the instrument under ambient temperature. Triplicate measurements were performed for each sample. Results were analyzed by affiliated Dispersion Technology Software.

2.7.2. Morphology

Morphology of the nanocrystals was observed by JSM-6701F scanning electron microscope (SEM, JEOL, Tokyo, Japan) at accelerating voltage of 10 kV. The samples were filtrated by the 50 nm filter membrane. The membrane was air-dried and fixed onto the stub. The PTX powder was directly fixed onto the stub. Both samples were sputter-coated with conductive layers of gold for 1 min at the current of 20 mA before the SEM observation.

2.7.3. Solid state characterization

To evaluate the solid state characteristics of PTX nanocrystals, the obtained nanosuspensions were freeze-dried. Power X-ray diffraction (PXRD) was collected on an AXS D8 Advance powder diffractometer (Bruker Corp., Karlsruhe, Germany) with Cu K_α radiation (40 kV, 60 mA). Scans were obtained from 3° to 60° with step size of 0.02° and scan rate of 0.3°/min. Differential scanning calorimeter (DSC) (Q2000, TA Instruments, Ghent, Belgium) was also used to determine the degree of crystallinity of PTX nanocrystals. Samples, 5 mg, were placed in a hermetically closed aluminum pan. The heating rate of the scanning calorimeter was 5 K/min, from 50 to 320 °C.

2.8. In-vitro dissolution studies

In vitro dissolution behavior of PTX nanocrystals was conducted in 0.5% (*w/v*) Tween 80 aqueous solution. The dissolution was conducted in a ZRS-8G dissolution tester (Tianda Tianfa Technology Co., Ltd., Tianjin, China) according to Chinese Pharmacopeia Method III. Briefly, samples equivalent to 1.2 mg PTX were added to 200 mL dissolution media stirred at 100 rpm and maintained at 37 ± 0.5 °C. Two milliliters were withdrawn at predetermined intervals of 5, 10, 15, 30, 45, 60, 90 and 120 min, respectively, from the vessel, being replaced with equal volume of blank medium. Collected samples were filtrated through 50 nm membrane and analyzed with HPLC. HPLC conditions were the same as the above mentioned except adjusted linear range. The PTX concentration was linear with peak area within concentration range from 0.051 to 10.12 μg/mL. A typical calibration curve was $C = 0.0264A - 0.0269$ ($r^2 = 0.9998$).

3. Results and discussion

3.1. Metastable zone of PTX in ethanol aqueous solutions

Fig. 2 shows the effects of ethanol concentrations on the solubility of PTX. When the concentration of ethanol exceeded 30%, the solubility of PTX was significantly increased. Additionally, the ethanol concentration had even more pronounced effects on the metastable limit of PTX. When the ethanol concentration exceeded

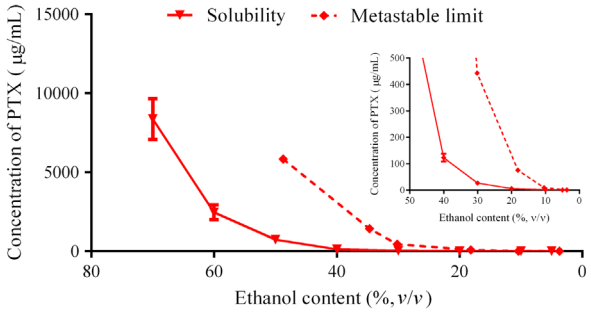

Figure 2 Metastable zone of PTX in ethanol aqueous solutions (inset: enlargement in the ethanol range of 0–50% and PTX concentration range of 0–500 μg/mL).

10%, larger increase in the metastable limit was obtained, as compared with the increase in solubility, (Fig. 2 inset). A wide metastable zone is thus available for preparation of nanocrystals. To better control nucleation and minimize loss of PTX, metastable solutions with low ethanol concentration, such as around 20%, were presently used to prepare nanocrystals.

3.2. *Preparation of nanocrystals*

3.2.1. *Screen of composition of metastable solution*

Metastable concentration of PTX in different ethanol aqueous solutions for preparation of nanocrystals was first explored. For ease of comparison, the metastable solutions were only subjected to sonication process for nucleation, without any post-treatments steps such as filtration and redispersion. The particle size and PDI of the obtained suspensions were measured (Table 1). Both the PTX concentration and ethanol content showed pronounced effects on the particle size and PDI of the nanocrystals. Although higher PTX concentrations can be achieved at higher ethanol content such as 22%, the obtained nanocrystals were in the micrometer range with a broad size distribution. When the ethanol content was decreased to 16% and PTX concentration less than 30 μg/mL, nanocrystals with a size around 550 nm could be obtained. Minor alterations of the ethanol content also caused several fold changes in metastable limit while retaining similar solubility, significantly affecting the supersaturation. High supersaturation at a high ethanol content facilitated nucleation and produced more crystal nuclei. Aggregation of the nuclei may result in larger crystals instead of nanocrystals. Nonetheless, it is very difficult to obtain nanocrystals smaller than 500 nm, likely due to Ostwald Ripening. Ethanol is a good solvent for PTX and may promote the Ostwald ripening compared with pure water. Facilitated by sonication, small nanocrystals may dissolve while the bigger ones grow. In this respect, it is thus critical to remove ethanol after the nucleation process.

3.2.2. *Optimization of sonication processes*

Metastable solution of 30 μg/mL PTX in 16% ethanol aqueous solution was used to optimize sonication conditions. A metastable solution was first triggered by sonication to induce nucleation. After respective 15, 30, and 45 min of sonication, the resulting suspensions were filtered through 50 nm membranes. The filter cake was redispersed in 5 mL pure water under sonication. Variations in particle size during the redispersing process was recorded (Table 2). Both the particle size and PDI of nanocrystals tend to be decreased along with the redispersing process in pure water, indicating that smaller and more uniform nanocrystals were obtained (Figs. 3 and 4). The sonication time in the nucleation stage also influenced the particle size of the final nanocrystals. Nanocrystals produced by 15 min of sonication showed particle sizes ranging from 293 to 422 nm but with a broad and asymmetric size distribution (Fig. 3). Extending the sonication time to 30 and 45 min further decreased the particle size of the nanocrystals with a symmetrical size distribution (Fig. 4). Although nucleation was instantly triggered by the sonication process as PTX concentration was close to the metastable limit, crystal nuclei continued growing. If sonication was halted right after the formation of nuclei, the crystal nuclei would grow into elongated fibers (Fig. 5). On the contrary, continuous sonication could serve as an "annealing" process to reduce the aspect ratio of nanocrystals during the nucleation procedures[34]. Since there were no significant differences in sonication time between 30 and 45 min, the sonication times of nucleation and redispersing process were set to 30 and 15 min, respectively.

Table 1 Compositions of metastable solution and properties of corresponding nanocrystals.

Metastable solution		Sonication time in nucleation (min)	Size (nm)	PDI
Ethanol (%)	PTX (μg/mL)			
22	138	30	994.7	0.224
22	137	30	/	/
22	136	30	2109	0.175
22	135	45	/	/
20	77	30	/	/
20	75	30	1157	0.790
20	73	45	/	/
20	71	45	/	/
18	62	20	/	/
18	61	30	/	/
18	60	30	/	/
18	56	30	/	/
18	52	30	/	/
17	52	30	/	/
17	50	30	1012	0.366
17	48	30	824.6	0.104
17	46	30	/	/
17	44	45	837.6	0.423
17	40	45	835.7	0.217
17	38	45	/	/
17	34	45	/	/
16	40	30	609.7	0.402
16	38	30	969.3	0.281
16	38	45	721.7	0.311
16	38	70	761.7	0.363
16	34	45	750.0	0.314
16	32	45	885.6	0.642
16	30	15	483.5	0.245
16	30	30	554.3	0.281
16	30	45	648.5	0.241
16	28	15	591.7	0.194
16	28	30	525.5	0.224
16	28	45	563.0	0.141
16	25	45	/	/
14	25	15	/	
14	25	30	/	/

"/" means significant precipitations.

Table 2 Variation of particle size during the sonication process.

Sonication time in nucleation stage (min)	Sonication time for redispersion							
	1 min		5 min		10 min		15 min	
	Size (nm)	PDI	Size (nm)	PDI	Size (nm)	PDI	Size (nm)	PDI
15	422.2±7.351	0.285±0.024	359.8±9.840	0.165±0.014	303.4±4.067	0.173±0.035	293.5±3.172	0.233±0.069
30	268.1±5.600	0.224±0.060	241.0±3.262	0.188±0.006	227.8±4.579	0.175±0.019	218.7±5.508	0.149±0.018
45	262.8±14.46	0.269±0.067	230.9±4.104	0.132±0.018	238.3±2.354	0.186±0.015	243.4±6.265	0.147±0.009

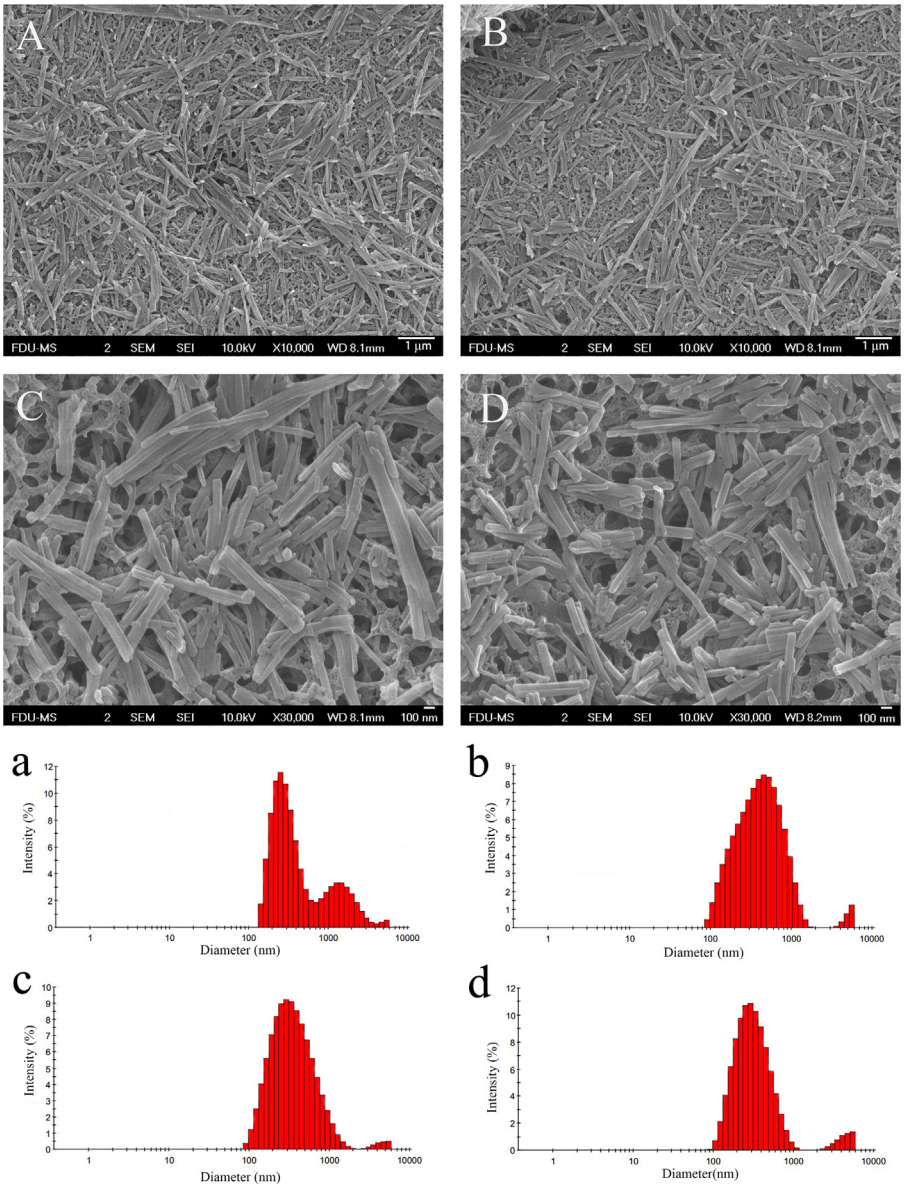

Figure 3 Metastable solution, 30 μg/mL PTX in 16% ethanol aqueous solution, was used to prepare nanocrystals. Sonication in nucleation stage lasted 15 min. The obtained nanosuspensions were filtered and redispersed in 5 mL pure water. SEM photographs (A)–(D) and size distribution (a)–(d) of PTX nanocrystals in redispersing process under sonication for (A) and (a) 1 min, (B) and (b) 5 min, (C) and (c) 10 min, and (D) and (d) 15 min.

3.2.3. Applicability of the technique

Based on the optimized sonication parameters, the range of the solution compositions that are suitable to prepare nanocrystals were studied (Table 3). A metastable solution was triggered by sonication for 30 min to induce nucleation. The ethanol aqueous solution was removed by filtration through 50 nm membrane. The

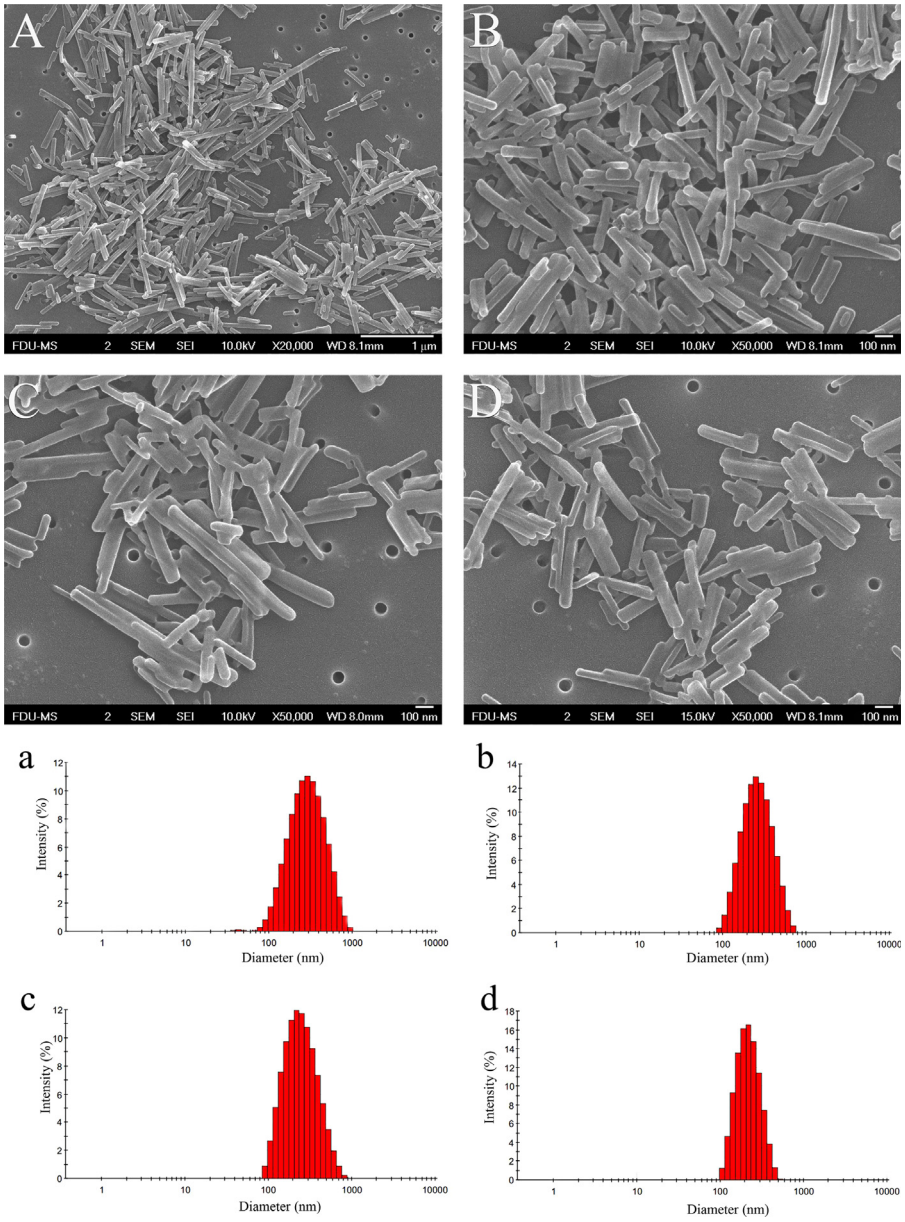

Figure 4 Metastable solution, 30 μg /mL PTX in 16% ethanol aqueous solution, was used to prepare nanocrystals. Sonication in nucleation stage lasted 30 min. The obtained nanosuspensions were filtered and redispersed in 5 mL pure water. (A)–(D) SEM photographs and (a)–(d) size distribution of PTX nanocrystals in redispersing process under sonication for (A) and (a) 1 min, (B) and (b) 5 min, (C) and (c) 10 min, and (D) and (d) 15 min.

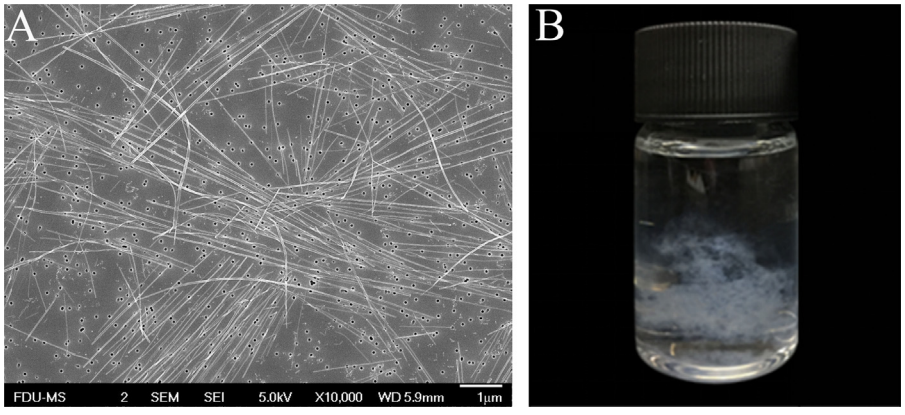

Figure 5 Crystal nuclei grow into tenuous fibers when sonication halted right after the formation of nuclei: (A) SEM photograph and (B) appearance.

Table 3 Size distribution of nanocrystals prepared with different metastable solutions.

Metastable solution		Sonication for redispersion					
		5 min		10 min		15 min	
Ethanol (%)	PTX (μg/mL)	Size (nm)	PDI	Size (nm)	PDI	Size (nm)	PDI
16	26	291.6	0.161	257.7	0.045	240.5	0.167
16	28	290.0	0.199	241.7	0.189	219.6	0.162
16	30	351.2	0.253	300.0	0.203	259.3	0.154
16	32	334.0	0.243	298.8	0.185	266.8	0.123
16	40	325.5	0.230	268.6	0.207	259.4	0.111
17	40	Large particles		Particles		411.4	0.306
17	45	274.8	0.228	301.2	0.148	262.6	0.217
17	50	323.7	0.250	310.8	0.131	298.4	0.121
18	52	350.1	0.240	297.9	0.197	256.8	0.167
18	56	Large particles		791.6	0.416	1379	0.844
18	60	Large particles		522.8	0.459	522.1	0.276
19	55	353.2	0.167	279.7	0.165	239.2	0.125
19	60	524.6	0.335	413.7	0.232	396.1	0.200
19	65	523.9	0.269	454.3	0.327	412.2	0.199
19	70	515.5	0.239	457.9	0.166	379.0	0.138
20	60	278.2	0.084	292.3	0.176	242.1	0.135
20	65	355.3	0.236	337.9	0.189	340.8	0.213
20	70	340.0	0.156	308.4	0.112	287.7	0.129
20	75	Large particles		Large particles		Large particles	
20	80	328.2	0.231	348.2	0.208	334.0	0.130
22	80	Particles		437.9	0.249	385.5	0.154
22	90	271.6	0.155	250.2	0.119	241.9	0.131
22	100	Large particles		464.7	0.248	437.8	0.178
22	110	615.8	0.304	567.0	0.161	666.3	0.356
25	90	389.5	0.221	370.6	0.236	366.7	0.205
25	100	Large particles		Particles		285.8	0.169
25	110	334.2	0.149	289.5	0.163	289.2	0.160
25	120	Large particles		Particles		316.4	0.160
25	140	Large particles		Large particles		Large particles	

filter cake was redispersed in 5 mL pure water under sonication for 15 min. The variation in particle size and PDI during the redispersion process was recorded (Table 3). Both the particle size and PDI was decreased as the sonication procedure proceeded. Nanocrystals were obtained in a wide range of compositions (Table 3). Typical compositions that may be adopted to prepare small and uniform carrier-free nanocrystals are shown in Fig. 6A. The PTX concentration was increased by 3-fold when ethanol content increased from 16% to 22%, indicating a significant improvement in production efficiency. The PTX concentration was still low compared with other bottom-up techniques[8–10]. This is ascribed to the limitation by the metastable method. Because the technique is simple and easy to control, scale-up can be achieved by parallel production. The yield of nanocrystals and recovery of PTX were also measured (Fig. 6B). The yield of nanocrystals was around 70%, while the recovery of PTX around 90%. The difference is due to the solubilization of PTX in the ethanol aqueous solution. The accumulation of crystal nuclei stops at the point where drug concentration decreases to its solubility. Drug loss is inevitable in this technique, which is one reason that high ethanol content cannot be used. However, lost drug can be recycled from the filtrate because no any other carrier materials are added.

3.3. *Characterization of PTX nanocrystals*

Due to the comparatively high yield, nanocrystals prepared from metastable solution of 90 μg/mL PTX in 22% ethanol aqueous solution were characterized. The preparation process is as follows: PTX was dissolved in 45% ethanol aqueous solution (10 mL) to a concentration of 0.184 mg/mL, which was maintained at 40 °C and agitated under 200 rpm; 10.45 mL water of equal temperature was instilled using a syringe pump at 160 μL/min to get the metastable solution; sonication was performed to the metastable solution to trigger nucleation; after 30 min of sonication, the obtained suspension was filtered through 50 nm membranes; the filter cake was redispersed in 5 mL pure water under sonication of 15 min.

The nanosuspensions were clear and transparent with light blue opalescence (Fig. 7A). The mean particle size was 241.9 ± 11.35 nm with a PDI value of 0.131 ± 0.026 (Fig. 7B). The PTX nanocrystals and raw materials are shown in Fig. 7C and D, respectively. Raw PTX were bulk crystals, while nanocrystals were acicular. The long dimension of the pure nanocrystals measured from SEM images was similar to that detected by Malvern Zetasizer Nano®. The majority of the nanocrystals were around 200 nm. A small quantity of elongated nanocrystals around 300 nm was observed due to the crystal growth. In addition,

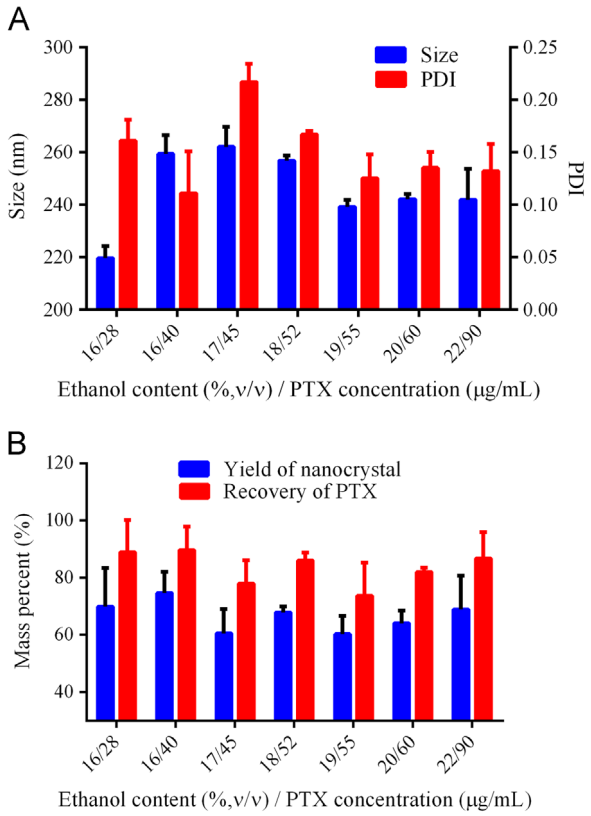

Figure 6 (A) Size distribution of nanocrystals prepared by a wide range of metastable compositions, and (B) the yield of nanocrystals and recovery of PTX.

because no stabilizers were used in the preparation, the boundaries of the nanocrystals appeared regular.

Lyophilization showed little impact on the particle size and PDI of the processed nanocrystals. The particle size and PDI of freeze-dried nanocrystals were 264.5 ± 9.57 and 0.207 ± 0.03, respectively. PXRD patterns of PTX raw material and nanocrystals are shown in Fig. 8A, where PXRD peaks of the raw PTX were detected at 5.5°, 10.0°, 12.2°, and 13.9°, indicating paclitaxel dehydrate[35,36]. All of these characteristic diffraction peaks are observed of PTX nanocrystal samples as well, indicating no alteration of crystallinity of PTX. DSC thermograms of the raw materials and nanocrystals are shown in Fig. 8B. The raw material displayed an endothermic peak at 220.2 °C, corresponding to its melting point[37]. However, no such endothermic peak was observed of PTX nanocrystals. Instead, only an exothermal peak was detected at 215.2 °C, suggesting PTX decomposition. Since particle size can have a significant effect on nanomaterial decomposition, these results suggest that the decomposition temperature of the nanocrystal product may be lowered at smaller particle size[38]. The exothermic peak may conceal the endothermic peak. An additional endothermic peak around 160 °C was seen in both PTX raw materials and nanocrystals, indicating solid–solid transition[35]. followed by dehydration shown by a broad endothermic peak around 100 °C. Nonetheless, the crystalline status of PTX nanocrystals was confirmed by the results of PXRD and DSC.

3.4. *In vitro drug dissolution*

Dissolution profiles of PTX raw material and nanocrystals are shown in Fig. 9. Dissolution was significantly enhanced by nanocrystals comparing with the raw material. About 82% of

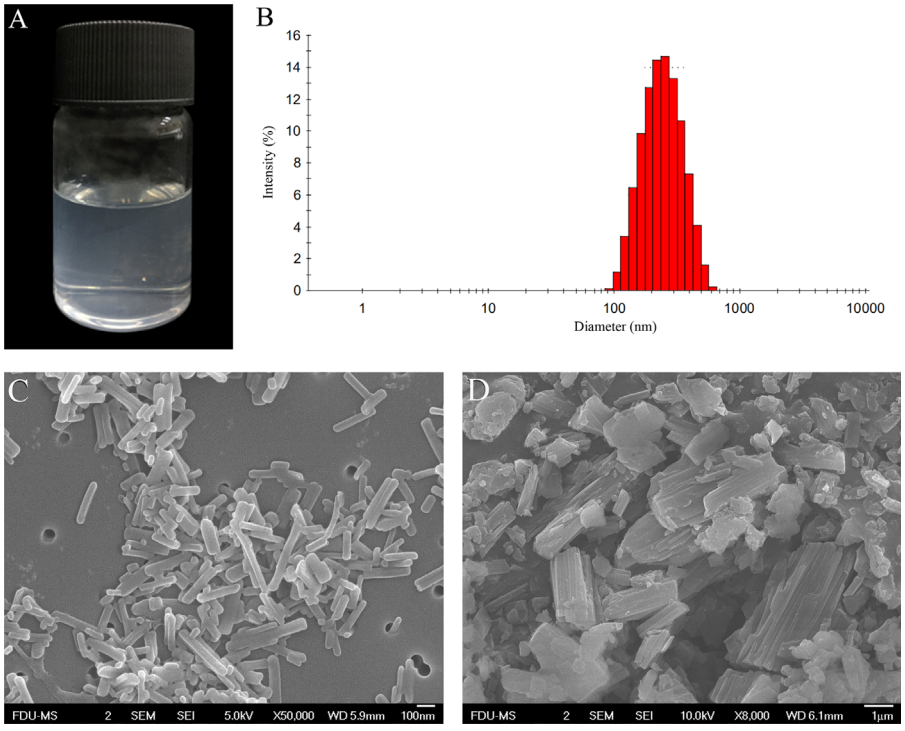

Figure 7 (A) The appearance, (B) the size distribution and SEM photographs of (C) PTX nanocrystals prepared from metastable solution of 90 μg/mL PTX in 22% ethanol aqueous solution. (D) SEM photographs of PTX raw materials.

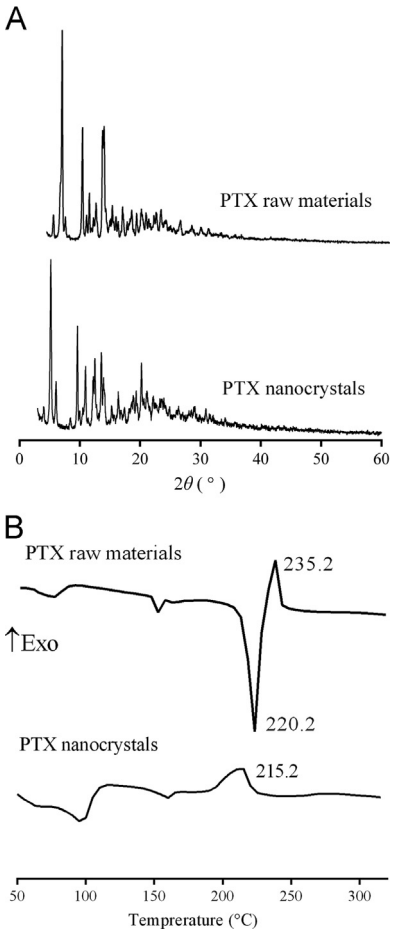

Figure 8 (A) PXRD patterns and (B) DSC of PTX raw material and nanocrystals.

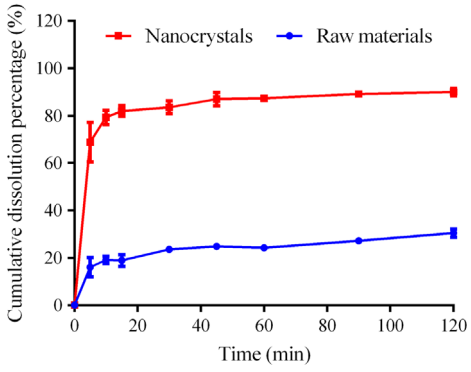

Figure 9 *In vitro* dissolution of PTX raw materials and nanocrystals in 0.5% Tween 80 aqueous solution ($n=3$).

added PTX nanocrystals was dissolved in 15 min, while only 18.9% was dissolved of the raw material. The enhanced dissolution of PTX by nanocrystals can be explained by Noyes–Whitney equation[1,2,5]. As shown in Fig. 7, the raw PTX bears a particle size ranging from several to a dozen micrometers. It is estimated that a 500-fold increase in total surface area can be achieved by reducing the particle size from 10 μm to 200 nm[39]. Meanwhile, the apparent solubility of nanoparticles is increased according to the Ostwald–Freundlich equation[40]. The increase in surface area together with the enhancement in solubility due to the particle size reduction leads to increased dissolution rate of PTX.

The present study provides a new strategy to prepare carrier-free nanocrystals. The process is quite simple and easy of control. However, limited by the metastable method, the concentration of nanocrystals is lower than other bottom-up techniques. It is essential to concentrate the nanocrystals prior to post-processing. Tangential flow filtration may be appropriate for this purpose. A parallel production strategy is practicable for scale-up. Moreover, it should be noted that nanocrystals are an intermediate product. Development of proper dosage form is prerequisite for clinic use. Close attention should be paid to the size stability during formulation preparation and storage. In general, the presently-described technique shows great potential to prepare carrier-free nanocrystal preparations.

4. Conclusions

Experiments to optimize production of PTX nanocrystals found that variations in ethanol concentration influenced the metastable limits of PTX than more significantly than PTX solubility, providing a wide metastable zone that can be used for preparation of carrier-free nanocrystals. Nucleation may be triggered by sonication from the metastable zone. Present results found that it is critical to remove ethanol from the system after nucleation to generate smaller nanocrystals. It is also important to redisperse these preparations by sonication to control the particle size and size distribution of the resulting PTX nanocrystals. The presently-described PTX nanocrystals dissolved significantly better than PTX raw material. These results demonstrate the importance of nucleation in producing organic nanocrystals and describe a feasible approach to prepare uniform carrier-free nanocrystals.

Acknowledgements

This work was supported by the Natural Science Foundation of Shanghai (16ZR1403500).

References

1. Lu Y, Chen Y, Gemeinhart RA, Wu W, Li T. Developing nanocrystals for cancer treatment. *Nanomedicine* 2015;**10**:2537–52.
2. Lu Y, Li Y, Wu W. Injected nanocrystals for targeted drug delivery. *Acta Pharm Sin B* 2016;**6**:106–13.
3. Xie Y, Shi B, Xia F, Qi J, Dong X, Zhao W, et al. Epithelia transmembrane transport of orally administered ultrafine drug particles evidenced by environment sensitive fluorophores in cellular and animal studies. *J Control Release* 2017;**270**:65–75.
4. Shen C, Yang Y, Shen B, Xie Y, Qi J, Dong X, et al. Self-discriminating fluorescent hybrid nanocrystals: efficient and accurate tracking of translocation via oral delivery. *Nanoscale* 2017;**10**:436–50.
5. Lu Y, Qi J, Dong X, Zhao W, Wu W. The *in vivo* fate of nanocrystals. *Drug Discov Today* 2017;**22**:744–50.
6. Pramanick S, Singodia D, Chandel V. Excipient selection in parenteral formulation development. *Pharma* 2013;**45**:65–77.
7. Zhang H, Hollis CP, Zhang Q, Li T. Preparation and antitumor study of camptothecin nanocrystals. *Int J Pharm* 2011;**415**:293–300.
8. Zhao R, Hollis CP, Zhang H, Sun L, Gemeinhart RA, Li T. Hybrid nanocrystals: achieving concurrent therapeutic and bioimaging functionalities toward solid tumors. *Mol Pharm* 2011;**8**:1985–91.
9. Hollis CP, Weiss HL, Leggas M, Evers BM, Gemeinhart RA, Li T. Biodistribution and bioimaging studies of hybrid paclitaxel nanocrystals: lessons learned of the EPR effect and image-guided drug delivery. *J Control Release* 2013;**172**:12–21.

10. Hollis CP, Weiss HL, Evers BM, Gemeinhart RA, Li T. *In vivo* investigation of hybrid paclitaxel nanocrystals with dual fluorescent probes for cancer theranostics. *Pharm Res* 2014;**31**:1450–9.
11. Zhang H, Wang X, Dai W, Gemeinhart RA, Zhang Q, Li T. Pharmacokinetics and treatment efficacy of camptothecin nanocrystals on lung metastasis. *Mol Pharm* 2014;**11**:226–33.
12. Xia D, Gan Y, Cui F. Application of precipitation methods for the production of water-insoluble drug nanocrystals: production techniques and stability of nanocrystals. *Curr Pharm Des* 2014;**20**:408–35.
13. Kwon SG, Hyeon T. Formation mechanisms of uniform nanocrystals via hot-injection and heat-up methods. *Small* 2011;**7**:2685–702.
14. Sugimoto T. Underlying mechanisms in size control of uniform nanoparticles. *J Colloid Interface Sci* 2007;**309**:106–18.
15. Sosso GC, Chen J, Cox SJ, Fitzner M, Pedevilla P, Zen A, et al. Crystal nucleation in liquids: open questions and future challenges in molecular dynamics simulations. *Chem Rev* 2016;**116**:7078–116.
16. Wang LY, Zhu L, Yang LB, Wang YF, Sha ZL, Zhao XY. Thermodynamic equilibrium, metastable zone widths, and nucleation behavior in the cooling crystallization of gestodene-ethanol systems *J Cryst Growth* 2016;**437**:32–41.
17. Bhoi S, Sarkar D. Modelling and experimental validation of ultrasound assisted unseeded batch cooling crystallization of L-asparagine monohydrate. *CrystEngComm* 2016;**18**:4863–74.
18. Zhang XY, Yang ZQ, Chai J, Xu JY, Zhang L, Qian G, et al. Nucleation kinetics of lovastatin in different solvents from metastable zone widths. *Chem Eng Sci* 2015;**133**:62–9.
19. Dalvi SV, Dave RN. Analysis of nucleation kinetics of poorly water-soluble drugs in presence of ultrasound and hydroxypropyl methyl cellulose during antisolvent precipitation. *Int J Pharm* 2010;**387**:172–9.
20. Dalvi SV, Yadav MD. Effect of ultrasound and stabilizers on nucleation kinetics of curcumin during liquid antisolvent precipitation. *Ultrason Sonochem* 2015;**24**:114–22.
21. Hollis CP, Li T. Nanocrystals production, characterization, and application for cancer therapy. In: Yeo Y, editor. *Nanoparticulate drug delivery systems: strategies, technologies, and applications*. New York: John Wiley & Sons, Inc; 2013. p. 181–206.
22. Ji JB, Lu XH, Xu ZC. Effect of ultrasound on adsorption of geniposide on polymeric resin. *Ultrason Sonochem* 2006;**13**:463–70.
23. Thanki K, Gangwal RP, Sangamwar AT, Jain S. Oral delivery of anticancer drugs: challenges and opportunities. *J Control Release* 2013;**170**:15–40.
24. Mazzaferro S, Bouchemal K, Ponchel G. Oral delivery of anticancer drugs I: general considerations. *Drug Discov Today* 2013;**18**:25–34.
25. Luo C, Sun J, Du Y, He Z. Emerging integrated nanohybrid drug delivery systems to facilitate the intravenous-to-oral switch in cancer chemotherapy. *J Control Release* 2014;**176**:94–103.
26. Wong J, Brugger A, Khare A, Chaubal M, Papadopoulos P, Rabinow B, et al. Suspensions for intravenous (IV) injection: a review of development, preclinical and clinical aspects. *Adv Drug Deliv Rev* 2008;**60**:939–54.
27. Zhang T, Luo J, Fu Y, Li H, Ding R, Gong T, et al. Novel oral administrated paclitaxel micelles with enhanced bioavailability and antitumor efficacy for resistant breast cancer. *Colloids Surf B Biointerfaces* 2017;**150**:89–97.
28. Zabaleta V, Ponchel G, Salman H, Agueros M, Vauthier C, Irache JM. Oral administration of paclitaxel with pegylated poly(anhydride) nanoparticles: permeability and pharmacokinetic study. *Eur J Pharm Biopharm* 2012;**81**:514–23.
29. Cheng Q, Shi H, Huang H, Cao Z, Wang J, Liu Y. Oral delivery of a platinum anticancer drug using lipid assisted polymeric nanoparticles. *Chem Commun (Camb)* 2015;**51**:17536–9.
30. Wei W, Lv P, Ma G. Oral delivery of protein and anticancer drugs by uniform-sized chitosan micro/nanoparticles with autofluorescent property. *J Control Release* 2015;**213**:e111.
31. Mazzaferro S, Bouchemal K, Ponchel G. Oral delivery of anticancer drugs III: formulation using drug delivery systems. *Drug Discov Today* 2013;**18**:99–104.
32. Sangwal K, Mielniczek-Brzoska E. Antisolvent crystallization of aqueous ammonium dihydrogen phosphate solutions by addition of methanol. *J Cryst Growth* 2016;**451**:139–49.
33. Sangwal K, Mielniczek-Brzóska E. Antisolvent crystallization of aqueous ammonium dihydrogen phosphate solutions by addition of acetone at different rates. *Cryst Res Technol* 2016;**51**:475–90.
34. Xu Y, Liu X, Lian R, Zheng S, Yin Z, Lu Y, et al. Enhanced dissolution and oral bioavailability of aripiprazole nanosuspensions prepared by nanoprecipitation/homogenization based on acid-base neutralization. *Int J Pharm* 2012;**438**:287–95.
35. Liggins RT, Hunter WL, Burt HM. Solid-state characterization of paclitaxel. *J Pharm Sci* 1997;**86**:1458–63.
36. Zhao R, Hollis CP, Zhang H, Sun L, Gemeinhart RA, Li T. Hybrid nanocrystals: achieving concurrent therapeutic and bioimaging functionalities toward solid tumors. *Mol Pharm* 2011;**8**:1985–91.
37. Patel K, Patil A, Mehta M, Gota V, Vavia P. Oral delivery of paclitaxel nanocrystal (PNC) with a dual Pgp-CYP3A4 inhibitor: preparation, characterization and antitumor activity. *Int J Pharm* 2014;**472**:214–23.
38. Fathollahi M, Pourmortazavi SM, Hosseini SG. Particle size effects on thermal decomposition of energetic material. *J Energ Mater* 2007;**26**:52–69.
39. Mueller RH, Gohla S, Keck CM. State of the art of nanocrystals—special features, production, nanotoxicology aspects and intracellular delivery. *Eur J Pharm Biopharm* 2011;**78**:1–9.
40. Kesisoglou F, Panmai S, Wu Y. Nanosizing-oral formulation development and biopharmaceutical evaluation. *Adv Drug Deliv Rev* 2007;**59**:631–44.